Lecture 17: Optical Bloch equations

- Optical Bloch equations, Bloch sphere
- Time evolution of the Bloch vector

Optical Bloch equations: Having identified the role of the parameters Γ and $\delta\omega$ in the effective equations of motion for the atomic flip operators, Eqs. (16.4) and (16.5), we will attempt to solve these equations. First note that the evolution of the atomic flip operators is determined by the time dependence of the free electric field. Suppose now that $\hat{\mathbf{E}}_{\rm free}(\mathbf{r}_A)$ represents a monochromatic field with frequency ω_λ that has been prepared in a coherent state $|\alpha_\lambda\rangle$. Recall from the definition of the coherent states that, when taking the expectation value of the field in this state, we have to replace $2\langle\alpha_\lambda|\hat{\mathbf{E}}^{(+)}_{\rm free}(\mathbf{r}_A)|\alpha_\lambda\rangle\cdot\mathbf{d}/\hbar \mapsto i\Omega e^{-i\omega_\lambda t}$ where

$$\Omega = \frac{2\omega_\lambda \alpha_\lambda}{\hbar}\mathbf{A}_\lambda(\mathbf{r}_A)\cdot\mathbf{d} \tag{17.1}$$

is the *Rabi frequency*. Although it has the dimension of a frequency, it is in general a complex quantity and measures the strength of the atom-light interaction.

We now absorb the fast (free) time dependence $e^{-i\omega_\lambda t}$ by rewriting Eqs. (16.4) and (16.5) in a frame co-rotating with frequency ω_λ. By re-defining $\hat{\sigma} = e^{-i\omega_\lambda t}\hat{\tilde{\sigma}}$ we then obtain (we omit the ˜ sign again)

$$\dot{\hat{\sigma}} = -i\delta\hat{\sigma} + \frac{\Omega}{2}\hat{\sigma}_z - \frac{\Gamma}{2}\hat{\sigma}\,, \tag{17.2}$$

$$\dot{\hat{\sigma}}_z = -\Gamma(1+\hat{\sigma}_z) - \Omega\hat{\sigma}^\dagger - \Omega^*\hat{\sigma}\,, \tag{17.3}$$

where we defined the *detuning* $\delta = \omega_A + \delta\omega - \omega_\lambda$.

The effective equations of motion for the atomic transition operators are not very helpful if one tries to understand the atomic evolution. However, they can be converted into c-number differential equations by taking the trace over the atomic density matrix. Recall that the expectation value of an operator $\hat{O}$ is given by $\langle\hat{O}\rangle = \mathrm{Tr}(\hat{\varrho}\hat{O})$. Here the operator $\hat{O}$ is in fact a time derivative of one of the $\hat{\sigma}_i$. Hence, an expectation value of the type $\langle\dot{\hat{\sigma}}_i\rangle = \mathrm{Tr}[\hat{\varrho}\dot{\hat{\sigma}}_i]$ is being computed in the Heisenberg picture in which the operators carry the time dependence. In contrast, in the Schrödinger picture, it is the density operator, i.e. the quantum state, that varies in time. However, expectation values can be computed in both pictures and they give the same answer. We thus seek to compute $\langle\dot{\hat{\sigma}}_i\rangle = \mathrm{Tr}[\dot{\hat{\varrho}}\hat{\sigma}_i]$.

The density operator of a two-level atom is, written in the $\{|g\rangle, |e\rangle\}$-basis, a Hermitian 2×2-matrix. The space of Hermitian 2×2-matrices is spanned by the identity matrix in that space and the three Pauli matrices (these matrices form a basis into which all matrices can be expanded). This means that the density matrix of any two-level system can be written in the form

$$\hat{\varrho} = \frac{1}{2}\left(\hat{I} + \mathbf{u}\cdot\hat{\boldsymbol{\sigma}}\right) \tag{17.4}$$

where $\mathbf{u} = (u, v, w)^T$ is a real vector with norm $|\mathbf{u}| \leq 1$ and $\hat{\boldsymbol{\sigma}}$ is the vector of Pauli matrices. Due to the trace properties of the Pauli matrices, $\mathrm{Tr}(\hat{\sigma}_i\hat{\sigma}_j) = 2\delta_{ij}$, the elements of the vector $\mathbf{u}$ are given by

$$u_i = \mathrm{Tr}(\hat{\varrho}\hat{\sigma}_i)\,. \tag{17.5}$$

In particular, with our definitions of the Pauli matrices, $u = \mathrm{Tr}[\hat{\varrho}(\hat{\sigma}+\hat{\sigma}^\dagger)]$, $v = i\mathrm{Tr}[\hat{\varrho}(\hat{\sigma}-\hat{\sigma}^\dagger)]$ and $w = \mathrm{Tr}(\hat{\varrho}\hat{\sigma}_z)$. The expression (17.4) converts the (Hermitian) density matrix into a real vector inside a three-dimensional ball.

Obviously, u and v are just the real and imaginary parts, respectively, of the off-diagonal atomic matrix elements. Then we can rewrite Eqs. (17.2) and (17.3) as

$$\boxed{\begin{pmatrix}\dot{u}\\ \dot{v}\\ \dot{w}\end{pmatrix} = \begin{pmatrix}0 & -\delta & \Omega_R\\ \delta & 0 & -\Omega_I\\ -\Omega_R & \Omega_I & 0\end{pmatrix}\begin{pmatrix}u\\ v\\ w\end{pmatrix} - \frac{\Gamma}{2}\begin{pmatrix}u\\ v\\ 2(1+w)\end{pmatrix}}\,. \tag{17.6}$$

This set of equations is called *optical Bloch equations* and it describes the motion of the *Bloch vector* $\mathbf{u} = (u, v, w)^T$ on the *Bloch sphere*. In order to gain some insight into Eq. (17.6), we have a look at what particular values of the Bloch vector mean physically. By its definition, the vector $\mathbf{u}^T = (0, 0, -1)$, i.e. the south pole of the Bloch sphere, represents the ground state $|g\rangle$ of the atom, and the vector $\mathbf{u}^T = (0, 0, 1)$ pointing towards the north pole represents the excited state $|e\rangle$. A vector in the equatorial plane with $w = 0$ must therefore be a superposition of $|e\rangle$ and $|g\rangle$ whose phase is determined by u and v. It is easy to verify that an atomic state $|\psi_A\rangle = (|e\rangle + e^{i\varphi}|g\rangle)/\sqrt{2}$ yields $u = \langle\psi_A|\hat{\sigma} + \hat{\sigma}^\dagger|\psi_A\rangle = \cos\varphi$ and $v = \langle\psi_A|i(\hat{\sigma} - \hat{\sigma}^\dagger)|\psi_A\rangle = \sin\varphi$.

Time evolution of the Bloch vector: The time evolution of the Bloch vector is determined by the Rabi frequency Ω and the detuning δ from the resonance. For zero detuning and negligible spontaneous decay, the external driving field simply causes the atom to flop

between its ground and excited states with the Rabi frequency. Starting in the ground state $|g\rangle$, i.e. with the initial conditions $u(0) = 0, v(0) = 0, w(0) = -1$, the solutions to the Bloch equations read

$$u(t) = -\sin\Omega t\,, \quad v(t) = 0\,, \quad w(t) = -\cos\Omega t\,, \qquad (\Gamma = \delta = 0)\,. \tag{17.7}$$

This process is called *Rabi flopping* and is depicted in Figure 22 (red curve).

We see that we can bring the atom into a coherent superposition state $\propto |e\rangle + e^{i\phi}|g\rangle$ if the interaction time is chosen to be exactly $t = \pi/(2\Omega)$. Because the azimuthal angle of the Bloch vector changes by $\pi/2$ during this evolution, this process is called a $\pi/2$-pulse. If the interaction time is chosen to be $t = \pi/\Omega$, one transfers the population completely into the excited state $|e\rangle$ (π-pulse).

FIG. 22: Time evolution of the Bloch vector for different detunings δ and $\Gamma = 0$ (left figure). The values starting with the red curve are: $\delta = 0,\ 0.5,\ 1,\ 2,\ 3$. The Rabi frequency was set to $\Omega = 1$. Time evolution of the Bloch vector with $\Gamma = 0.2$. The other parameters are $\delta = 0.5$ and $\Omega = 1$.

For non-zero detuning, the Bloch vector precesses on a cone starting from the south pole of the Bloch sphere with an opening angle that is determined by δ (see Figure 22),

$$\begin{aligned} u(t) &= -\frac{\Omega}{\sqrt{\delta^2+\Omega^2}}\sin\sqrt{\delta^2+\Omega^2}t\,, \\ v(t) &= -\frac{\delta\Omega}{\delta^2+\Omega^2}(1-\cos\sqrt{\delta^2+\Omega^2}t)\,, \\ w(t) &= -1+\frac{\Omega^2(1-\cos\sqrt{\delta^2+\Omega^2}t)}{\delta^2+\Omega^2}\,, \end{aligned} \tag{17.8}$$

with a precession frequency $\sqrt{\delta^2+\Omega^2} > \Omega$. We can see why if we look at the first term on the right of Eq. (17.6) which we can write as a vector product

$$\dot{\mathbf{u}} = \boldsymbol{\beta} \times \mathbf{u}\,, \quad \boldsymbol{\beta} = \begin{pmatrix} \Omega_I \\ \Omega_R \\ \delta \end{pmatrix}\,. \tag{17.9}$$

Differential equations such as Eq. (17.9) appear already in classical physics as the equation of motion of the gyroscope or spinning top. The Bloch vector $\mathbf{u}$ precesses, starting from its initial state, around the vector $\boldsymbol{\beta}$. For zero detuning and real Rabi frequency, the vector $\boldsymbol{\beta}$ points in the v-direction and the Bloch vector describes a great circle in the (u,w)-plane (red curve in left panel of Fig. 22).

Note that in the above examples, because Γ has been set to zero, the Bloch vector is of unit length, $|\mathbf{u}| = 1$ which, by Eq. (17.4), means that the atom is in a pure state for all times. Obviously, because spontaneous decay is always present, the atomic density matrix will in general be mixed and the Bloch vector will have a length $|\mathbf{u}| < 1$. The right panel in Fig. 22 shows a typical evolution of the Bloch vector starting from the ground state $|g\rangle$ until the steady-state value is reached.

Stationary solutions of the Bloch equations: Finally, we will have a look at the stationary solutions of Eq. (17.6). They are characterized by the condition $\dot{\mathbf{u}} = \mathbf{0}$. For simplicity, let us assume that the Rabi frequency Ω is real. Then we find that

$$u_{\rm stat} = -\frac{\delta\Omega}{\frac{\Omega^2}{2}+\delta^2+(\frac{\Gamma}{2})^2}\,, \quad v_{\rm stat} = -\frac{\frac{\Gamma}{2}\Omega}{\frac{\Omega^2}{2}+\delta^2+(\frac{\Gamma}{2})^2}\,, \quad w_{\rm stat} = -1+\frac{\frac{\Omega^2}{2}}{\frac{\Omega^2}{2}+\delta^2+(\frac{\Gamma}{2})^2}\,. \tag{17.10}$$

In the limit when the driving is weak compared to the spontaneous decay rate, $\Omega \ll \Gamma$, we obtain from Eq. (17.10) that $w_{\rm stat} \approx -1$. This means that the atom resides closely to its ground state $|g\rangle$. In the opposite limit, when the driving dominates the restoring force, $\Omega \gg \Gamma$, and the frequency of the incoming radiation field is on resonance with the atomic transition, $\delta = 0$, then $w_{\rm stat} \approx 0$. In this case there is a roughly equal probability for finding the atom in its ground state $|g\rangle$ or in its excited state $|e\rangle$. However, for any values of the parameters, $w_{\rm stat}$ is strictly negative, $w_{\rm stat} < 0$, so that the probability to find the atom in its ground state is always larger than the excited-state probability. In other words, there is no steady-state solution for a two-level atom in which the atom is excited.

Lecture 18: Ramsey interferometer

- $\pi/2$-pulses revisited
- Stationary solutions to the Bloch equations

$\pi/2$**-pulses revisited**: Let us return to the Bloch equations (17.6) and recall their solutions in the absence of spontaneous decay, $\Gamma = 0$, and vanishing detuning, $\delta = 0$. Starting at the south pole of the Bloch sphere, $\mathbf{u}^T(0) = (0, 0, -1)$, the solution is simply [see Eq. (17.7)]

$$\begin{aligned} u(t) &= -\sin\Omega t\,, \\ w(t) &= -\cos\Omega t\,, \end{aligned}$$

which corresponds to motion in the (u, w)-plane. After a time $t = \pi/(2\Omega)$, the Bloch vector performs a rotation around the v-axis by an angle $\pi/2$, $\mathbf{u}^T(\pi/2) = (-1, 0, 0)$. The result is an equal superposition of ground and excited states,

$$|\psi(\pi/2)\rangle = \frac{1}{\sqrt{2}}\left(|e\rangle - |g\rangle\right) \tag{18.1}$$

which lies on the equator of the Bloch sphere. Clearly, another $\pi/2$-pulse will bring the atom into its excited state $|e\rangle$.

All the states on the equator of the Bloch sphere are equal superpositions of $|e\rangle$ and $|g\rangle$, albeit with different relative phases between them. Consider now a situation in which an external perturbation induces a motion along the equator. In our gyroscopic picture this corresponds to a rotation around the w-axis which can only be generated by a perturbation Hamiltonian of the form

$$\hat{H}_{\rm pert} = \hbar g \hat{\sigma}_z \tag{18.2}$$

that generates a time evolution

$$\hat{U}_{\rm pert}(t) = e^{-igt\hat{\sigma}_z} = \cos(gt) - i\sin(gt)\hat{\sigma}_z\,. \tag{18.3}$$

Applied to the state (18.1) gives

$$\hat{U}_{\rm pert}(t)|\psi(\pi/2)\rangle = \frac{1}{\sqrt{2}}\left(e^{-igt}|e\rangle - e^{igt}|g\rangle\right) = \frac{1}{\sqrt{2}}\left[\cos(gt)\left(|e\rangle - |g\rangle\right) - i\sin(gt)\left(|e\rangle + |g\rangle\right)\right]\,. \tag{18.4}$$

This rotates the Bloch vector by an azimuthal angle $\varphi = gt$ around the equator to the position $\mathbf{u}^T = (-\cos(gt), \sin(gt), 0)$.

If we now apply a second $\pi/2$-pulse, we do not necessarily end up in the excited state anymore. Instead, the final state after the pulse will be

$$|\psi\rangle = \cos(gt)|e\rangle - i\sin(gt)|g\rangle\,. \tag{18.5}$$

A subsequent projective measurement in the $\{|g\rangle, |e\rangle\}$-basis will show that the atom is in its ground state with probability $p_g = \sin^2(gt)$ and in the excited state with probability $p_e = \cos^2(gt)$. Such a measurement can be performed by irradiating the atom with radiation that is capable of ionizing only the excited state and, in a second step, with radiation that ionizes also a ground-state atom. This is the basic principle behind the *Ramsey interferometer* (see Fig. 23) which finds a wide range of applications in quantum optics and atomic physics.

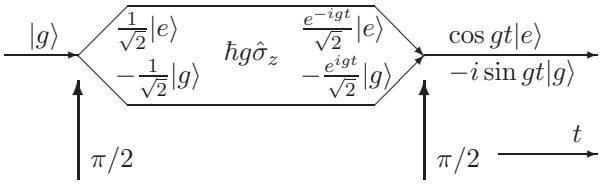

FIG. 23: Schematic Ramsey interferometer. The separate paths are internal states, not external degrees of freedom. See description in the text.

Let us comment on the sensitivity of the Ramsey interferometer. As before with the Mach–Zehnder interferometer, we will estimate the phase error that one makes in such a measurement. The signal in the Ramsey interferometer is the expectation value of $\hat{\sigma}_z$,

$$\langle\hat{\sigma}_z\rangle = \cos^2(gt) - \sin^2(gt) = \cos(2gt)\,. \tag{18.6}$$

The noise, i.e. the uncertainty in a single measurement, is then

$$\sqrt{\langle(\Delta\hat{\sigma}_z)^2\rangle} = \sqrt{1-\cos^2(2gt)} = |\sin(2gt)|\,. \tag{18.7}$$

The phase sensitivity for a single measurement, Eq. (11.7), is thus

$$\Delta\varphi = \frac{\sqrt{\langle(\Delta\hat{\sigma}_z)^2\rangle}}{\left|\frac{\partial\langle\hat{\sigma}_z\rangle}{\partial(2gt)}\right|} = 1\,. \tag{18.8}$$

If we perform N independent measurements, i.e. we let a stream of N independent atoms pass through the interferometer, the signal strength increases by a factor N. The noise,

however, increases only by a factor $\sqrt{N}$ which we can show as follows. Let $\hat{\sigma}_z^{(i)}$ be the inversion operator associated with the ith atom. Then the total variance is

$$\begin{aligned}\left\langle \left(\sum_{i=1}^{N} \hat{\sigma}_z^{(i)} \right)^2 \right\rangle - \left\langle \sum_{i=1}^{N} \hat{\sigma}_z^{(i)} \right\rangle^2 &= \sum_{i=1}^{N} \left\langle \left(\hat{\sigma}_z^{(i)}\right)^2 \right\rangle + \sum_{i \neq j} \langle \hat{\sigma}_z^{(i)} \hat{\sigma}_z^{(j)} \rangle - \sum_{i=1}^{N} \left\langle \hat{\sigma}_z^{(i)} \right\rangle^2 - \sum_{i \neq j} \langle \hat{\sigma}_z^{(i)} \rangle \langle \hat{\sigma}_z^{(j)} \rangle \\ &= \sum_{i=1}^{N} \left\langle \left(\hat{\sigma}_z^{(i)}\right)^2 \right\rangle - \sum_{i=1}^{N} \left\langle \hat{\sigma}_z^{(i)} \right\rangle^2 = N \left| \sin(2gt) \right| . \end{aligned} \tag{18.9}$$

Here we have used that $\langle \hat{\sigma}_z^{(i)} \hat{\sigma}_z^{(j)} \rangle = \langle \hat{\sigma}_z^{(i)} \rangle \langle \hat{\sigma}_z^{(j)} \rangle$ because we assumed that the measurements are all independent. Combining these results we find that the phase noise of N independent measurements is

$$\Delta\varphi = \frac{1}{\sqrt{N}} \tag{18.10}$$

which shows the same scaling as the Mach–Zehnder interferometer. The difference in the interpretation is that in Ramsey interferometry N denotes the number of atoms, whereas in Mach–Zehnder interferometry $\bar{n}$ is the average number of photons in the coherent state.

The Mach–Zehnder interferometer for photons (see lecture 11) uses matter in the form of beam splitters to create two separate paths for the photons. In the Ramsey interferometer it is light in the form of $\pi/2$-pulses that forces the atom into different 'paths'. This latter type of interferometer is peculiar in that there is no separate spatial pathways that the atom takes. The 'objects' that pick up the phases or phase differences are the two internal states $|g\rangle$ and $|e\rangle$. However, we will see in a later lecture that the absorption and emission of a photon is connected with a change of momentum which could then be used to indeed force the atom into separate pathways.

Lecture 19: Resonance fluorescence

- Intensity of the scattered light
- Intensity correlations, photon anti-bunching
- squeezing in resonance fluorescence

Intensity of the scattered light: If a two-level atom is driven by an external radiation field, we have seen that the atom periodically absorbs and emits photons. The emitted (or scattered) light from the driven atom can be collected at a photodetector. The measurement of the intensity of the scattered light reveals details of the nature of the atom-light interaction.

Let us recall the equation of motion (15.15) for the photonic amplitude operators,

$$\dot{\hat{a}}_\lambda = -i\omega_\lambda \hat{a}_\lambda + \frac{\omega_\lambda}{\hbar}\mathbf{A}^*_\lambda(\mathbf{r}_A)\cdot\mathbf{d}^*\hat{\sigma}\,,$$

and let us again integrate it with respect to time as in Eq. (16.1),

$$\hat{a}_\lambda(t) = e^{-i\omega_\lambda t}\hat{a}_\lambda + \frac{\omega_\lambda}{\hbar}\mathbf{A}^*_\lambda(\mathbf{r}_A)\cdot\mathbf{d}^*\int dt'\,\Theta(t-t')e^{-i\omega_\lambda(t-t')}\hat{\sigma}(t')\,.$$

Inserting this solution into the expression for the electric-field strength, we obtain for the positive frequency components

$$\hat{\mathbf{E}}^{(+)}(\mathbf{r},t) = \hat{\mathbf{E}}^{(+)}_{\rm free}(\mathbf{r},t) + i\sum_\lambda \frac{\omega_\lambda^2}{\hbar}\left[\mathbf{A}_\lambda(\mathbf{r})\otimes\mathbf{A}^*_\lambda(\mathbf{r}_A)\right]\cdot\mathbf{d}^*\int dt'\,\Theta(t-t')e^{-i\omega_\lambda(t-t')}\hat{\sigma}(t')\,. \quad (19.1)$$

We can rewrite this expression as

$$\hat{\mathbf{E}}^{(+)}(\mathbf{r},t) = \hat{\mathbf{E}}^{(+)}_{\rm free}(\mathbf{r},t) + \int dt'\,\Theta(t-t')\boldsymbol{G}(\mathbf{r},t;\mathbf{r}_A,t')\cdot\mathbf{d}^*\hat{\sigma}(t')\,, \quad (19.2)$$

where the propagator function

$$\boldsymbol{G}(\mathbf{r},t;\mathbf{r}_A,t') = i\sum_\lambda \frac{\omega_\lambda^2}{\hbar}\left[\mathbf{A}_\lambda(\mathbf{r})\otimes\mathbf{A}^*_\lambda(\mathbf{r}_A)\right]e^{-i\omega_\lambda(t-t')} \quad (19.3)$$

propagates an excitation from the space-time point $(\mathbf{r}_A,t')$ to $(\mathbf{r},t)$.

At the moment, we are not interested in the details of this propagator function. However, in view of the Markov approximation discussed earlier, we introduce the slowly-varying

atomic operators $\hat{\sigma}(t') = e^{-i\omega_A t'}\hat{\tilde{\sigma}}(t')$ and take them at the retarded time $t - |\mathbf{r} - \mathbf{r}_A|/c$ outside the time integral,

$$\hat{\mathbf{E}}^{(+)}(\mathbf{r},t) = \hat{\mathbf{E}}^{(+)}_{\rm free}(\mathbf{r},t) + \hat{\sigma}(t - |\mathbf{r}-\mathbf{r}_A|/c)\int dt'\,\Theta(t-t')e^{i\omega_A(t-|\mathbf{r}-\mathbf{r}_A|/c-t')}\boldsymbol{G}(\mathbf{r},t;\mathbf{r}_A,t')\cdot\mathbf{d}^*\,. \tag{19.4}$$

If we now let $t \to \infty$ under the integral, the resulting function $\mathbf{g}(\mathbf{r},\mathbf{r}_A)$ is an effective propagator and the electric-field strength can finally be written as

$$\hat{\mathbf{E}}^{(+)}(\mathbf{r},t) = \hat{\mathbf{E}}^{(+)}_{\rm free}(\mathbf{r},t) + \mathbf{g}(\mathbf{r},\mathbf{r}_A)\hat{\sigma}(t - |\mathbf{r}-\mathbf{r}_A|/c)\,. \tag{19.5}$$

Since the photocurrent at a photodetector is proportional to the light intensity, we have to compute $I(\mathbf{r},t) = \langle \hat{\mathbf{E}}^{(-)}(\mathbf{r},t)\cdot\hat{\mathbf{E}}^{(+)}(\mathbf{r},t)\rangle$ with the electric-field strength given by Eq. (19.5). Because we are interested only in the contribution from the scattered light, we obtain

$$I(\mathbf{r},t) = |\mathbf{g}(\mathbf{r},\mathbf{r}_A)|^2\langle\hat{\sigma}^\dagger(t-|\mathbf{r}-\mathbf{r}_A|/c)\hat{\sigma}(t-|\mathbf{r}-\mathbf{r}_A|/c)\rangle\,. \tag{19.6}$$

But the expectation value of the product of atomic operators is nothing but the excited-state probability $(1+w)/2$ taken at the retarded time. Hence, the observed intensity reflects the dynamics of the optical Bloch equations.

In the limit of zero detuning, the excited-state probability can be computed to be

$$\sigma_{ee}(t) = \frac{\Omega^2}{2\Omega^2+4\Gamma^2}\left[1 - e^{-3\Gamma t/2}\left(\cosh\sqrt{(\tfrac{\Gamma}{2})^2-\Omega^2}t + \frac{3\Gamma\sinh\sqrt{(\tfrac{\Gamma}{2})^2-\Omega^2}t}{2\sqrt{(\tfrac{\Gamma}{2})^2-\Omega^2}}\right)\right]\,. \tag{19.7}$$

In the limit of a weak driving field, $\Omega^2 \ll \Gamma^2$, we obtain for the intensity

$$I_{\rm weak}(\mathbf{r},t+|\mathbf{r}-\mathbf{r}_A|/c) = |\mathbf{g}(\mathbf{r},\mathbf{r}_A)|^2\frac{\Omega^2}{\Gamma^2}\left(1-e^{-\Gamma t/2}\right)^2 \tag{19.8}$$

which approaches the steady-state solution $|\mathbf{g}(\mathbf{r},\mathbf{r}_A)|^2\Omega^2/\Gamma^2$ that can be read off from Eq. (17.10). In the opposite limit of strong driving, $\Omega^2 \gg \Gamma^2$, we obtain

$$I_{\rm strong}(\mathbf{r},t+|\mathbf{r}-\mathbf{r}_A|/c) = \frac{1}{2}|\mathbf{g}(\mathbf{r},\mathbf{r}_A)|^2\left(1-e^{-3\Gamma t/4}\cos\Omega t\right) \tag{19.9}$$

which oscillates with the Rabi frequency Ω. These oscillations are damped on a time scale given by the spontaneous decay rate Γ (see Fig. 24).

Intensity correlations, photon anti-bunching: In order to describe the statistics of the scattered light, we need to look at the intensity correlation function. As we saw, the function

$$G^{(2)}(\mathbf{r},t+\tau,\mathbf{r},t) = \langle\hat{E}_i^{(-)}(\mathbf{r},t)\hat{E}_j^{(-)}(\mathbf{r},t+\tau)\hat{E}_j^{(+)}(\mathbf{r},t+\tau)\hat{E}_i^{(+)}(\mathbf{r},t)\rangle \tag{19.10}$$

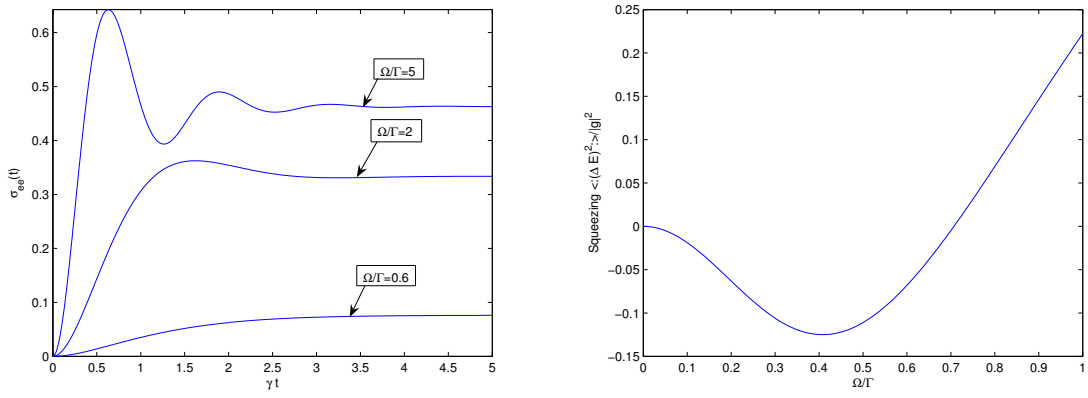

FIG. 24: Time evolution of the excited-state probability $\sigma_{ee}(t)$ for different ratios Ω/Γ (left figure). Squeezing in resonance fluorescence (right figure).

can be used to infer whether a given quantum state of light shows nonclassical behaviour such as photon anti-bunching. With the expression (19.5) for the electric-field strength, we find that $[r = |\mathbf{r} - \mathbf{r}_A|]$

$$\begin{aligned} G^{(2)}(\mathbf{r}, t + r/c + \tau, \mathbf{r}, t + r/c) &= |\mathbf{g}(\mathbf{r}, \mathbf{r}_A)|^4 \langle \hat{\sigma}^\dagger(t) \hat{\sigma}^\dagger(t+\tau) \hat{\sigma}(t+\tau) \hat{\sigma}(t) \rangle \\ &= |\mathbf{g}(\mathbf{r}, \mathbf{r}_A)|^4 \langle \hat{\sigma}^\dagger(t) \hat{\sigma}_{ee}(t+\tau) \hat{\sigma}(t) \rangle \,. \end{aligned} \tag{19.11}$$

In the coincidence limit, $\tau = 0$, we find that $G^{(2)}(\mathbf{r}, t + r/c, \mathbf{r}, t + r/c) = 0$. This means that the joint probability of registering two photons at the same time in the detectors vanishes and indicates perfect photon anti-bunching. The steady-state intensity correlation function $G^{(2)}(\tau) = \lim_{t\to\infty} G^{(2)}(\mathbf{r}, t + r/c + \tau, \mathbf{r}, t + r/c)$ therefore must have a positive initial slope,

$$G^{(2)}(\tau) > G^{(2)}(0) = 0 \,. \tag{19.12}$$

To understand the origin of photon anti-bunching in resonance fluorescence, we can invoke the following intuitive picture. A driven two-level atom can only emit a photon if it had been previously excited by the driving field. Once it emits a photon, the atom jumps back to its ground state. Hence, in other to emit a second photon, it must be re-excited by the driving field which takes a certain amount of time. Therefore, the atom cannot emit two photons at the same time, and the scattered light shows perfect photon anti-bunching.

Squeezing in resonance fluorescence: We have already seen that the scattered light from a resonantly driven two-level atom shows nonclassical behaviour in terms of photon

anti-bunching. But there is even more to it. The resonance fluorescence light can even be squeezed. To see that, recall that a measure for the occurence of squeezing is that the variance of the electric-field strength drops below the vacuum level for a particular choice of phase or, equivalently, if the normally-ordered variance of the electric-field strength becomes negative, $\langle : [\Delta\hat{\mathbf{E}}(\mathbf{r},t)]^2 : \rangle < 0$.

Using the source-quantity representation (19.5), we can write this variance as

$$\begin{aligned}\langle : [\Delta\hat{\mathbf{E}}(\mathbf{r},t+r/c)]^2 : \rangle &= 2|\mathbf{g}(\mathbf{r},\mathbf{r}_A)|^2\sigma_{ee}(t) \\ &\quad - \left[2|\mathbf{g}(\mathbf{r},\mathbf{r}_A)|^2|\sigma(t)|^2 + \mathbf{g}^2(\mathbf{r},\mathbf{r}_A)\sigma^2(t) + \mathbf{g}^{*2}(\mathbf{r},\mathbf{r}_A)\sigma^{*2}(t)\right] . \quad (19.13)\end{aligned}$$

Now we introduce again the slowly-varying amplitudes $\sigma(t) = e^{-i\omega_A t}\tilde{\sigma}(t)$ and write the product $\mathbf{g}(\mathbf{r},\mathbf{r}_A)\sigma(t)$ as $|\mathbf{g}(\mathbf{r},\mathbf{r}_A)\tilde{\sigma}(t)|\, e^{-i\omega_A t + i\varphi(t)}$ where $\varphi(t)$ denotes the sum of the phase of $\tilde{\sigma}(t)$ and the propagator function. Note that for vanishing detuning we have $\omega_A = \omega_\lambda$. Hence it follows that the variance is

$$\langle : [\Delta\hat{\mathbf{E}}(\mathbf{r},t+r/c)]^2 : \rangle = 2|\mathbf{g}(\mathbf{r},\mathbf{r}_A)|^2 \left\{\sigma_{ee}(t) - |\tilde{\sigma}(t)|^2\left[1+\cos 2(\omega_\lambda t - \varphi(t))\right]\right\} . \quad (19.14)$$

Recall from Eqs. (17.10) that the stationary values for large times $t \to \infty$ are simply

$$\sigma_{ee}(t) = \frac{1+w(t)}{2} \overset{t\to\infty}{\to} \frac{\Omega^2}{2\Omega^2+\Gamma^2}, \quad |\tilde{\sigma}(t)|^2 = \frac{u^2(t)+v^2(t)}{4} \overset{t\to\infty}{\to} \frac{\Gamma^2\Omega^2}{(2\Omega^2+\Gamma^2)^2}, \quad (19.15)$$

so that finally

$$\langle : [\Delta\hat{\mathbf{E}}(\mathbf{r},t+r/c)]^2 : \rangle \overset{t\to\infty}{\to} \frac{2\Omega^2}{(2\Omega^2+\Gamma^2)^2}|\mathbf{g}(\mathbf{r},\mathbf{r}_A)|^2\Big[2\Omega^2 - \Gamma^2\cos 2(\omega_\lambda t - \varphi(\infty))\Big] . \quad (19.16)$$

Since the trigonometric function in Eq. (19.16) is bounded by one, we can infer that the fluorescence light will be squeezed (for particular values of the phase) if

$$\boxed{\langle : [\Delta\hat{\mathbf{E}}(\mathbf{r},t+r/c)]^2 : \rangle < 0 \Longleftrightarrow 2\Omega^2 < \Gamma^2} . \quad (19.17)$$

This means that the driving field should not be too strong if one is to observe squeezing. The reason is that squeezing is a coherent effect which can only be built up if the atomic coherences $\sigma(t)$ play a significant role. However, in the strong-field limit the steady-state value of $\sigma(\infty)$ vanishes and the resonance fluorescence radiation is purely incoherent and squeezing is not observed. The maximally obtainable squeezing value is, for $\Omega = \Gamma/\sqrt{6}$, $\langle : [\Delta\hat{\mathbf{E}}(\mathbf{r},t+r/c)]^2 : \rangle = -|\mathbf{g}(\mathbf{r},\mathbf{r}_A)|^2/8$ (see right panel in Fig. 24).